

# TartanGround: A Large-Scale Dataset for Ground Robot Perception and Navigation

Manthan Patel<sup>1</sup>, Fan Yang<sup>1</sup>, Yuheng Qiu<sup>2</sup>, Cesar Cadena<sup>1</sup>, Sebastian Scherer<sup>2</sup>,  
Marco Hutter<sup>1</sup> and Wenshan Wang<sup>2</sup>

**Abstract**—We present TartanGround, a large-scale, multi-modal dataset to advance the perception and autonomy of ground robots operating in diverse environments. This dataset, collected in various photorealistic simulation environments includes multiple RGB stereo cameras for 360-degree coverage, along with depth, optical flow, stereo disparity, LiDAR point clouds, ground truth poses, semantic segmented images, and occupancy maps with semantic labels. Data is collected using an integrated automatic pipeline, which generates trajectories mimicking the motion patterns of various ground robot platforms, including wheeled and legged robots. We collect 878 trajectories across 63 environments, resulting in 1.44 million samples. Evaluations on occupancy prediction and SLAM tasks reveal that state-of-the-art methods trained on existing datasets struggle to generalize across diverse scenes. TartanGround can serve as a testbed for training and evaluation of a broad range of learning-based tasks, including occupancy prediction, SLAM, neural scene representation, perception-based navigation, and more, enabling advancements in robotic perception and autonomy towards achieving robust models generalizable to more diverse scenarios. The dataset and codebase are available on the webpage: <https://tartanair.org/tartanground>

## I. INTRODUCTION

Ground robots are increasingly being used in a wide range of environments, from structured urban areas to unstructured terrains such as forests, farmlands, and construction sites. These robots serve various purposes, including autonomous delivery, agricultural automation, industrial inspection, search-and-rescue missions, and construction site monitoring. To improve their adaptability and generalizability in these diverse settings, data-driven methods have gained traction. These approaches tackle key tasks in perception and scene understanding, such as Simultaneous Localization and Mapping (SLAM), occupancy prediction, semantic segmentation, monocular depth estimation, etc, enabling robots to better interpret, interact, and navigate their surroundings.

In the domain of autonomous driving, large-scale datasets [1]–[4] have played a crucial role in advancing machine learning models for tasks such as object detection, occupancy prediction, and semantic segmentation. These datasets offer standardized benchmarks that allow for consistent evaluation and comparison of algorithms. However, there is a notable lack of similar datasets and benchmarks for mobile robots operating in a broader range of environments. This absence makes it challenging to develop and evaluate generalizable models that can perform reliably across various and complex settings.

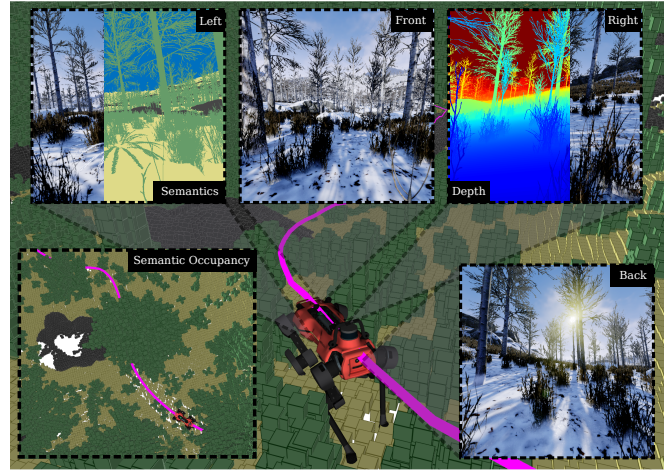


**Fig. 1:** A trajectory from TartanGround (Winter Forest environment) includes multiple stereo RGB images covering a full 360° field-of-view (fov), along with accurate depth and semantic annotations. It also provides ground truth poses, LiDAR, IMU data, and semantic occupancy maps for comprehensive scene understanding.

Several datasets support research in mobile robotics, each tailored to specific environments. For example, datasets [5]–[10] collected in off-road environments provide sensor modalities ranging from RGB cameras and LiDARs for scene understanding, to proprioceptive and traction data for vehicle dynamics modeling. Indoor datasets such as ScanNet [11], TUM RGB-D [12], and Matterport3D [13] provide RGB-D data for 3D reconstruction and SLAM. However, these datasets often have limitations in environmental diversity, size, accurate ground truths, or sensor types, which limit their applicability in developing robust, generalizable models.

Simulation datasets have become an important alternative to overcome these difficulties and limitations of real-world data collection in robotics. They offer a controlled environment for generating large-scale, high-quality data with precise ground truth annotations for semantics, depth, and poses—information that is often difficult to obtain in real-world settings. Furthermore, simulation enables diverse data collection under varying lighting, weather, and terrain conditions, improving model robustness and generalization. These benefits have made simulation datasets crucial for advancing perception tasks such as SLAM and monocular depth estimation. For instance, TartanAir [14] has been instrumental in training state-of-the-art (SoTA) SLAM algorithms like DROID-SLAM [15], demonstrating effective sim-to-real transfer. Similarly, synthetic datasets [16]–[18]

<sup>1</sup>Robotic Systems Lab, ETH Zurich, Zurich, Switzerland

<sup>2</sup>Robotics Institute of Carnegie Mellon University, Pittsburgh, USA

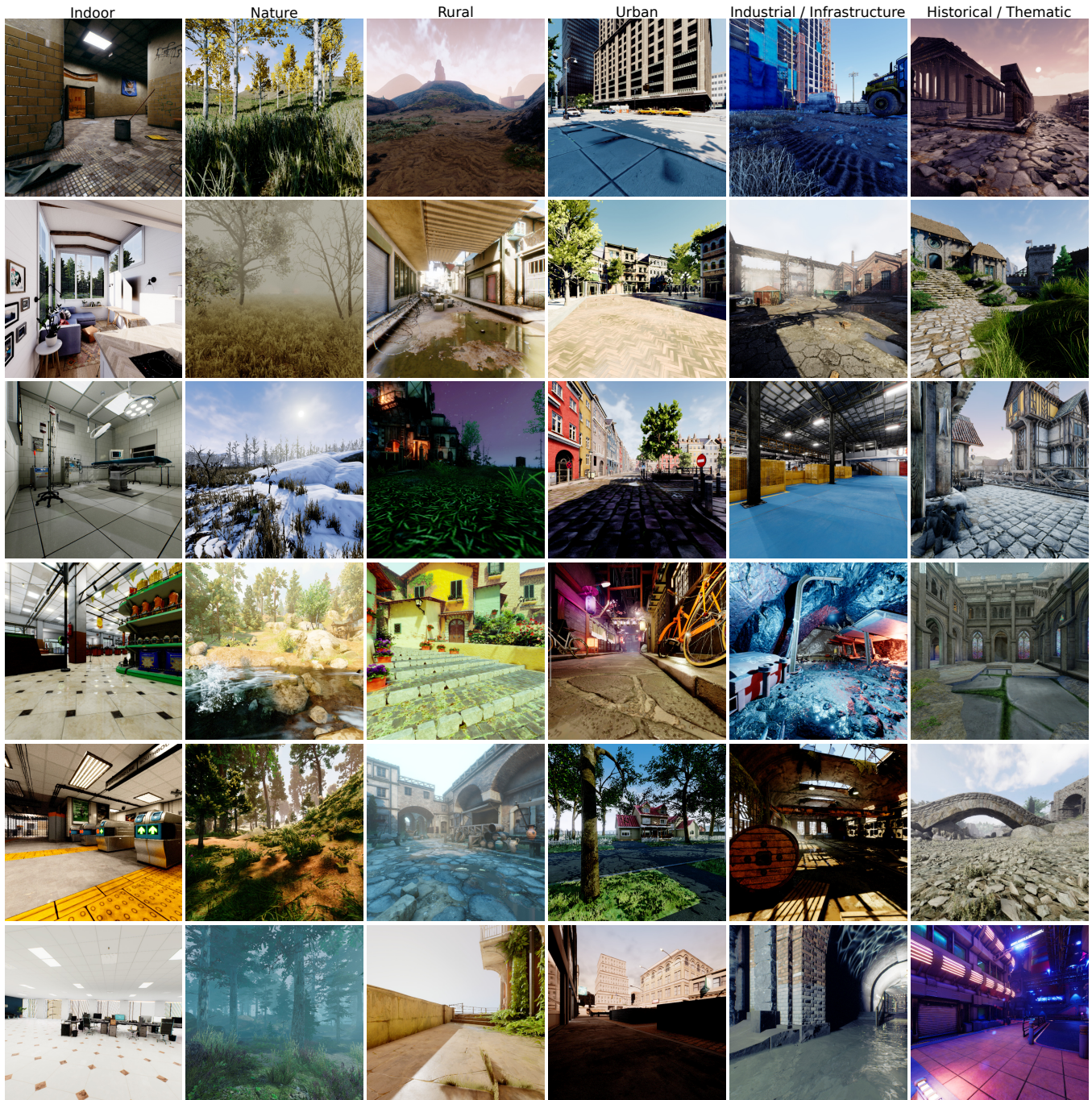


**Fig. 2:** The TartanGround environments, categorized into Indoor, Nature, Rural, Urban, Industrial/Infrastructure, and Historical/Thematic

have played a key role in training foundation models for monocular depth estimation [19], [20], further showcasing the impact of learning from simulation data.

To address the need for comprehensive data resources, we introduce TartanGround, a large-scale simulation dataset designed to support perception and navigation tasks for ground robots across diverse environments. TartanGround includes data from over 63 diverse, challenging photorealistic environments, offering multi-modal sensor data such as multiple stereo RGB-D images covering a 360°fov, semantic labels, LiDAR point clouds, semantic occupancy maps, and ground truth poses. We show that the existing SoTA occu-

pancy prediction methods, solely trained on data from the autonomous driving domain, do not generalize to environments of mobile robot operations such as forests. Moreover, we evaluate various SoTA SLAM algorithms and find that they struggle in challenging scenarios of low visibility and heavy occlusions. To summarize, the main contributions of this paper are: (1) A large dataset with over 1.44 million samples collected across diverse environments with precise ground truth labels mimicking different ground robot motion patterns, including wheeled (omnidirectional and differential-drive), and legged robots (quadrupedal), (2) an automatic data collection pipeline and (3) evaluation of two tasks,

occupancy prediction and SLAM highlighting the limitations of models trained on existing datasets.

## II. RELATED WORK

In the field of autonomous driving, the KITTI [1] dataset offers a comprehensive suite of sensor data, including stereo camera and LiDAR inputs, primarily for autonomous driving research. Building upon this, SemanticKITTI [21] extends KITTI by providing dense point-wise semantic labels for LiDAR scans, enabling advancements in LiDAR segmentation tasks. NuScenes [4] and Waymo Open Dataset [2] further contribute to urban scene understanding by offering 360° sensor coverage and diverse urban scenarios. Occ3D [22] establishes new benchmarks for semantic occupancy prediction on nuScenes and Waymo, facilitating the development of models that predict both the geometry and semantics of urban environments.

In indoor environments, several RGB-D datasets have been instrumental in advancing scene understanding. ScanNet [11] comprises annotated 3D reconstructions of indoor scenes, serving as a benchmark for tasks like 3D semantic segmentation and object recognition. TUM RGB-D [12] offers sequences recorded with handheld cameras, providing ground truth trajectories for evaluating SLAM and odometry algorithms. SUN RGB-D [23] and NYUv2 [24] provide paired RGB-D with semantic labels, supporting research in semantic segmentation and monocular depth estimation. Matterport3D [13] offers a rich collection of indoor images, facilitating research in 3D reconstruction and navigation.

For off-road environments, RELIS-3D [5] provides multi-modal data with dense annotations, supporting semantic segmentation research. RUGD [6] offers images captured in unstructured outdoor environments with pixel-wise semantic labels. GOOSE [7] presents data collected with a vehicle equipped with multiple cameras and LiDARs ensuring 360° coverage in offroad environments. WildScenes [10] provides synchronized image and LiDAR data with semantic annotations in natural settings, while TartanDrive [8] offers extensive sensor data for learning dynamics models in off-road driving scenarios. WildOcc [25] builds upon RELIS-3D by providing semantic occupancy annotations, enabling research in 3D scene understanding in off-road context.

Despite the significant contributions of these datasets, they are often limited by scale, environmental diversity, or sensor modalities, which can hinder the development of generalizable models for robotic perception and navigation. To address these limitations, TartanAir [14] introduced a large-scale synthetic dataset with 20 diverse environments and random motion patterns, enhancing generalization by offering photo-realistic imagery under varied weather and lighting conditions. TartanAir-V2 extended V1 with more scenes and more modalities [26]. Building on this, we introduce TartanGround, specifically targeting ground robots. It features realistic ground robot motion patterns, including wheeled and legged robots. We summarize the various datasets along with the sensor data, available ground truth, and scale in Tab. I. TartanGround is the only large-scale

dataset covering diverse environments and having realistic ground robot motions.

## III. THE DATASET

### A. Features

TartanGround consists of 63 realistic simulation environments from TartanAir-V2 [26], covering diverse scenarios from structured urban to large-scale unstructured outdoor environments (Fig. 2). The environments have been developed with Unreal Engine 4, and the data is collected using the AirSim [30] plugin. This setup allows for rendering photorealistic scenes with high fidelity and makes it possible to have dynamic lighting, adverse weather effects, dynamic objects, and seasonal changes. In each of the environments, we collect data from multiple sampled trajectories with diverse motion patterns mimicking real-world ground robots. To achieve full 360° coverage, we use 6 stereo RGB cameras (front, left, right, back, top, bottom), each with a fov of 90°. Each camera is synchronized with accurate ground truth poses and also records depth and semantic segmentation images. During post-processing, we generate additional ground truth data, including IMU data, optical flow, stereo disparity, LiDAR point clouds, and semantic occupancy maps. In total, we collect 878 trajectories (440 omni-wheeled, 198 diff-wheeled, and 240 legged), each with 600 to 8000 samples, resulting in a total dataset size of approximately 15 TB, 1.44 million samples, and 17.3 million RGB images. This large-scale, multi-modal dataset is designed to support a wide range of robotic perception and navigation tasks, benefiting the community in establishing new benchmarks for generalizable learning-based methods.

### B. Trajectory Sampling

The overview of the trajectory sampling pipeline is shown in Fig. 3.

1) *Environment Pointcloud*: We export the corresponding mesh (Fig. 3a) from Unreal Engine for each environment and sample a point cloud (Fig. 3b) with a specified density  $\delta$ . We exclude foliage elements such as grass and small bushes from the mesh export to ensure our geometry-based traversability estimation accurately reflects navigable paths. This approach allows us to generate trajectories that traverse compressible vegetation, capturing more realistic and diverse data.

2) *Traversability Generation*: We utilize a geometry-based traversability estimation pipeline inspired by [31], which, taking as an input the environment point cloud, can efficiently represent the environment with complex terrain conditions and spatial structures into 3D tomogram slices (Fig. 3c). This method extends traditional elevation maps [32] for multi-layered environments by assigning ground and ceiling elevations at fixed intervals, facilitating efficient planning of 3D trajectories for ground robots. Moreover, it incorporates the robot’s capabilities, such as climbing stairs and navigating steep gradients, by assessing factors like slope, step height, and overhead clearance to compute

**TABLE I:** Comparison of Datasets for Robotic Perception

Dataset	Type	Env	Motion Pattern	Stereo	Depth	LiDAR	Semantics	Occupancy	Pose	Multi-cam	Seq Num	Samples
Semantic KITTI [21]	Real	Urban	Car	✓	✗	✓	✓	✓	✓	✗	22	43 K
Occ3D-Waymo [2], [22]	Real	Urban	Car	✗	✗	✓	✓	✓	✓	5	1000	200 K
Occ3D-nuScenes [4], [22]	Real	Urban	Car	✗	✗	✓	✓	✓	✓	6	1000	40 K
RELLIS-3D [5]	Real	Off-road	Car	✓	✓	✓	✓	✗	✓	✗	5	6.2 K
RUGD [6]	Real	Off-road	Car	✗	✗	✗	✓	✗	✗	✗	18	7.5 K
TartanDrive [8]	Real	Off-road	Car	✓	✓	✗	✗	✗	✓	✗	630	184 K
WildScenes [10]	Real	Off-road	Hand	✗	✗	✓	✓	✗	✓	✗	5	9.6 K
WildOcc [25]	Real	Off-road	Car	✓	✓	✓	✓	✗	✓	✗	5	10 K
SynPhoRest [27]	Syn.	Off-road	Random	✗	✓	✓	✓	✗	✗	✗	X	3.1 K
GOOSE [7]	Real	Off-road	Car	✗	✗	✓	✓	✓	✓	4	356	10 K
GOOSE-Ex [28]	Real	Off-road	Tracked, Legged	✗	✗	✓	✓	✓	✓	4	100	5 K
Scannet [11]	Real	Indoor	Hand	✗	✓	✗	✓	✓	✓	✗	1500	2.5 M
GrandTour [29]	Real	Mix	Legged, Wheeled	✓	✓	✓	✗	✗	✓	3	100	100 K
TartanAir [14]	Syn.	Mix	Random	✓	✓	✗	✓	✗	✓	✗	1037	400 k
TartanAir-V2 [26]	Syn.	Mix	Random	✓	✓	✓	✓	✓	✓	6	1110	1.4 M
TartanGround	Syn.	Mix	Legged, Wheeled	✓	✓	✓	✓	✓	✓	6	878	1.4 M

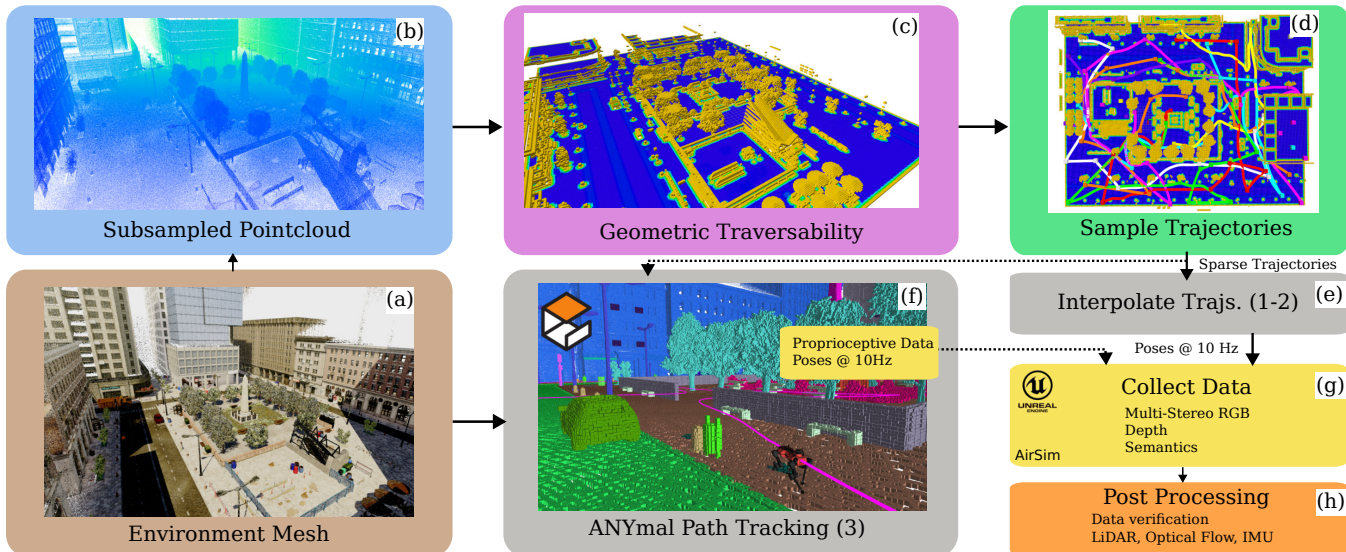


**Fig. 3:** Overview of the data collection pipeline. We first subsample a pointcloud (b) from the environment mesh (a), which is used to generate the geometric traversability (c). Next, we sample sparse long trajectories covering the environment, which are either interpolated to dense poses for wheeled robots (e) or used in a gazebo simulation with path tracking for quadrupeds (f) to generate the dense poses. The photorealistic data is then collected in AirSim using the poses (g), followed by a post-processing step (h).

the traversability values. This approach ensures robust performance in both structured and unstructured multi-layered environments.

3) *Sparse Trajectory Sampling*: Our objective is to generate  $\mathcal{S}$  long trajectories that maximize coverage of the environment while maintaining spatial diversity (Fig. 3d). To achieve this, we begin by uniformly sampling  $n/2$  points in free space and  $n/2$  points near obstacles, ensuring that the trajectories encompass both open and constrained regions. To eliminate redundancy, we apply a representative point sampling step using k-means clustering, resulting in a set of  $K$  representative points.

Each representative point is randomly assigned to one of the  $\mathcal{S}$  trajectory subgroups. For each subgroup, we construct a graph where nodes correspond to the sampled points and edges represent the path distance between them in the tomogram. We approximate the Traveling Salesman Problem (TSP) on this graph to determine an optimal traversal sequence. For each pair of consecutive nodes in the traversal sequence, we find the optimal smooth path using an A\* approach for tomograms [31]. The final path is obtained by

concatenating the subpaths between consecutive nodes, ensuring connectivity. This approach is summarized in Alg. 1. By the end of this process, we obtain  $\mathcal{S}$  sparse trajectories that provide comprehensive coverage of the environment.

4) *Dense Trajectory Generation*: To collect data in AirSim, we generate dense poses at a fixed frequency of 10 Hz, requiring realistic interpolation of sparse trajectories to accurately mimic ground robot motion while adhering to velocity and acceleration constraints. We implement three trajectory variations: (1) omnidirectional, (2) differential-drive (Fig. 3e), and (3) legged robot trajectories (Sec. III-C).

We use a fixed look-ahead distance for path tracking, ensuring the robot moves toward its tracking point. In omnidirectional motion, the robot can translate in any direction on the ground plane, meaning its heading may not always align with its movement direction. In contrast, the differential-drive model enforces a stricter motion constraint, requiring the robot to reorient itself to the next tracking point before proceeding. We apply a random walk model to introduce realistic velocity variations, adjusting speeds dynamically while sampling acceleration values within predefined lim-

---

**Algorithm 1** Sparse Trajectory Sampling

---

```
1: Input: Tomogram  $\mathcal{T}$ , samples  $n$ , trajectories  $\mathcal{S}$ 
2: Output: Sparse trajectories  $\mathcal{X} = \{X_1, X_2, \dots, X_S\}$ 
3:  $\mathcal{T}_{free} \leftarrow \text{SampleFreeSpace}(\mathcal{T}, n/2)$ 
4:  $\mathcal{T}_{obs} \leftarrow \text{SampleNearObstacles}(\mathcal{T}, n/2)$ 
5:  $\mathcal{T}_r \leftarrow \text{KMeans}(\mathcal{T}_{free} \cup \mathcal{T}_{obs}, K)$ 
6:  $\mathcal{S} \leftarrow \text{RandomAssign}(\mathcal{T}_r, S)$ 
7: for  $s \in \mathcal{S}$  do
8:    $G_s = (V_s, E_s)$ , where  $V_s = \mathcal{T}_r^s$ ,  $E_s = \text{path distances}$ 
9:    $\pi_s \leftarrow \text{SolveTSP}(G_s)$ 
10:  for  $(v_i, v_{i+1}) \in \pi_s$  do
11:     $P_{i,i+1} \leftarrow A^*(v_i, v_{i+1})$ 
12:     $X_s \leftarrow \text{Concat}(X_s, P_{i,i+1})$ 
13:  end for
14: end for
15: return  $\mathcal{X} = \{X_1, \dots, X_S\}$ 
```

---

its at each timestep. Additionally, we ensure smooth yaw transitions using a bounded yaw rate, maintaining physically plausible motion. We randomly sample the robot height in the range [0.5, 1.5] m for each trajectory. We also introduce Gaussian noise to the position to simulate real-world uncertainties, adding slight perturbations that account for terrain roughness and sensor and actuation inconsistencies.

### C. Legged Robot Trajectories

To capture realistic motion patterns of a legged robot, we perform path tracking of the sparse trajectories within a Gazebo simulation environment using an ANYmal D legged robot (Fig. 3f). An example of the ANYmal robot in action in a forest environment is shown in Fig. 1.

During simulation, we record the ground truth base poses, which are later used for sampling photorealistic data in AirSim. In addition to the base poses, we collect a comprehensive set of proprioceptive data, including base velocities and accelerations, joint states, and contact forces for each leg. In addition to the perception tasks, these trajectories can also be used for learning navigation tasks.

### D. Data Collection, Verification and Post-processing

For the provided dense poses (Fig. 3e-f), we capture 6 RGB stereo image pairs in AirSim, along with corresponding depth and semantic segmentation images. Using an approach similar to TartanAir [14], we generate additional ground truth data, including optical flow, stereo disparity, and simulated LiDAR measurements from these raw images. To enhance the usability of the dataset, we introduce a custom camera re-sampling feature that enables image extraction with arbitrary intrinsics and rotation matrices. This allows users to specify camera parameters that match their real robot setup, and the system re-renders images accordingly from the captured set of 6 images, ensuring compatibility with diverse robotic platforms.

For data verification, we ensure the synchronization between camera poses and captured images by computing the optical flow between consecutive image pairs and evaluating

the mean photometric error, as described in TartanAir [14]. Additionally, depth images are analyzed to verify collision occurrences with the environment.

## IV. EXPERIMENTS AND APPLICATIONS

In this section, we evaluate the performance of state-of-the-art methods on two key tasks: Occupancy Prediction and SLAM. We further discuss the other potential applications of the dataset.

### A. Occupancy Prediction

The task of predicting 3D occupancy voxels using multi-camera images has become quite popular in the field of autonomous driving as it enables detailed spatial representation of the environment useful for downstream tasks such as path planning and navigation. End-to-end occupancy prediction networks [22] have the advantage of handling occlusions and satisfying multi-camera consistency where traditional methods struggle. NuScenes [4] and Waymo [2] have become popular benchmarks for evaluating these learned networks, however, there is a lack of similar benchmarks for mobile robots operating in diverse environments. We show through experiments that the methods trained on autonomous driving data do not generalize to other environments, and thus, there is a need for such a large-scale dataset for training and evaluating in different scenes.

1) *Setup, Baselines, and Environments:* We set up two baselines for occupancy prediction. The first is a simple baseline that uses an off-the-shelf monocular depth estimator [20] to project pixels into 3D space using the predicted depth. To reduce the effect of bleeding artifacts, we further apply gradient filtering. This baseline is designed to highlight the limitations of depth-based projections and emphasize the need for dedicated occupancy prediction networks. Our second baseline is SurroundOcc [33], a state-of-the-art 3D occupancy prediction network. This network takes multiple RGB images as input and extracts per-image multi-scale features. Using 2D-3D spatial attention, the multi-camera information is fused to construct 3D multi-scale feature volumes which are decoded into semantic occupancy predictions.

For evaluating the baselines, we select three trajectories each from urban and natural environments, and truncate them to 1000 samples per trajectory. The urban environments depict city-like scenarios that are closer to the training domain of scenes (Fig. 4), while the natural environments include forest environments in different seasons and a marsh environment with heavy fog and low visibility. SurroundOcc network was trained on nuScenes data which was collected using a car mounted with six cameras having overlapping fov and facing front-left, front, front-right, back-left, back and back-right directions at a resolution of 1600x900 pixels. To minimize the domain gap, we re-render images matching this setup using our image resampling pipeline.

We use the Intersection over Union (IoU) metric to evaluate the performance of occupancy prediction. In principle, the network also predicts the semantic class along with



**Fig. 4:** (a) nuScenes urban environment (training data), (b) ModNeighborhood, (c) ForestAutumn, and (d) GreatMarsh, from TartanGround which exhibit increasing difference in distributions compared to the nuScenes.

**TABLE II:** Occupancy Prediction IoU ( $\uparrow$ )

Environment Name	Type	DepthPro [20]	SurroundOcc [33]
ModNeighborhood	Urban	17.29	<b>19.67</b>
OldtownSummer	Urban	17.37	<b>22.15</b>
NordicHarbor	Urban	11.62	<b>12.91</b>
ForestAutumn	Natural	<b>16.59</b>	13.89
ForestWinter	Natural	<b>16.97</b>	7.61
GreatMarsh	Natural	<b>12.04</b>	6.39

the occupancy, however, since the labels of nuScenes do not match our environment labels, we do not evaluate this. Moreover, instead of evaluating in the range of  $\pm 50$  m from the egocentric frame in x-y directions as in SurroundOcc, we only evaluate in the range of  $\pm 25$  m (at 0.5 m resolution) due to the relatively lower height of the cameras in our case limiting the longer distance visibility.

2) *Evaluations:* The quantitative results are summarized in Tab. II. In general, we observe that SurroundOcc outperforms the depth-based projection pipeline across all urban environments. This is expected since urban environments have a similar distribution as the nuScenes training dataset. Qualitative results for the ModNeighborhood environment are shown in Fig. 5. Here we see that SurroundOcc is able to predict the occupancy as well as the semantic classes (which we do not evaluate) for the car, vegetation, and driveable surface. On the other hand, visualizing the results of the depth projection method, we can clearly see the effect of bleeding and the inability to handle occlusions. Moreover, we also observe that this method suffers from inconsistent predictions across multiple views, leading to duplicating of objects when projected into 3D. These limitations highlight the advantages of occupancy prediction networks.

The natural environments are completely out-of-distribution for SurroundOcc, and thus, the performance in these environments is significantly lower than the urban environments. Moreover, these environments are also more challenging, with lower visibility and higher occlusion due to the presence of dense trees and tall grass. Interestingly, here, the depth projection method performs much better highlighting the generalization capabilities of the monocular depth-estimator network. We believe that our large-scale dataset can contribute towards the development of robust generalizable models for predicting semantic occupancy in diverse environments.

### B. Visual Odometry and SLAM

Visual Odometry (VO) and SLAM for ground robots pose unique challenges, such as vegetation occlusions, short

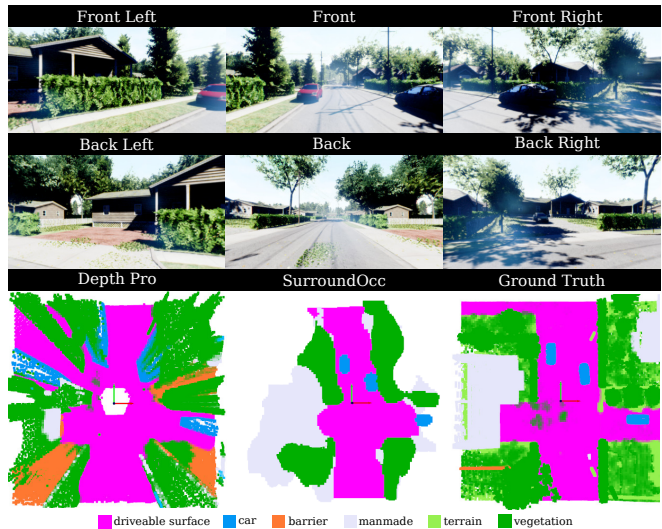


**Fig. 5:** Qualitative results for the Occupancy Prediction task from the ModNeighborhood environment. The Y-axis (green) points towards the front of the robot. The segmentation colors are for visualization purposes only. For the Depth-Pro method, segmentation is obtained using SAN [34] with the nuScenes labels as vocabulary.

horizon caused by low altitude, and aggressive motion due to bumpy terrain. TartanGround is designed to capture these challenging cases (as shown in Fig. 6). As a result, it becomes an interesting benchmark for VO and SLAM research.



**Fig. 6:** The environments used for testing SLAM, (a) Forest (heavy occlusion), (b) CastleFortress (indoor-outdoor transition), (c) WaterMillDay (running stream), (d) ModUrbanCity (dark stairs)

1) *Testing Environments and Baselines:* In this section, we show a small-scale evaluation of three state-of-the-art VO/SLAM algorithms on four challenging trajectories from four different environments. We use the front camera for these experiments. The trajectory from the Forest environment contains occlusion from tall grass and bushes, which are commonly presented in real-world off-road scenes. CastleFortress is a large scene with indoor-outdoor transitions, bringing dramatic illumination change. WaterMillDay has a rushing creek with water splash. ModUrbanCity contains a narrow dark stair that lacks good visual features. Our baseline consists of a classic geometry-based SLAM algorithm ORB-SLAM3 [35], a learning-based monocular odometry DPVO [36], and a stereo VO model MACVO [37]. We use relative translation error ( $t_{rel}$ , m/frame) and relative rotation error ( $r_{rel}$ ,  $^\circ$ /frame) to evaluate the results.

2) *Evaluation:* Table III presents the quantitative results of various VO/SLAM algorithms on the TartanGround trajectories. To ensure a fair comparison, we interpolate missing data points and concatenate successfully tracked segments when algorithms lose tracking. Among the evaluated al-

**TABLE III:** Performance comparison on the TartanGround Dataset.

Scenes	ORB-SLAM3 [35]		DPVO* <sup>†</sup> [36]		MAC-VO [37]	
	$t_{rel}$	$r_{rel}$	$t_{rel}$	$r_{rel}$	$t_{rel}$	$r_{rel}$
Forest	0.152	1.667	0.010	0.039	<b>0.008</b>	<b>0.038</b>
CastleFortress	0.338	1.943	0.031	<b>0.041</b>	<b>0.014</b>	0.070
WaterMill	0.404	1.090	0.089	<b>0.036</b>	<b>0.016</b>	0.062
ModUrban	0.563	2.742	0.030	<b>0.056</b>	<b>0.011</b>	0.099
<b>Average</b>	0.364	1.861	0.040	<b>0.043</b>	<b>0.012</b>	0.067

<sup>†</sup> Monocular method. \* Scale-aligned with ground truth.

**Fig. 7:** Novel view synthesis using Gaussian Splatting, trained on the Rome (a) and CoalMine (b) environments.

gorithms, ORB-SLAM3 frequently loses tracking, leading to significantly elevated translation and rotation errors. In contrast, MACVO and DPVO exhibit robustness across most environments. Notably, DPVO’s multi-frame design makes it more accurate in orientation estimation. However, its performance degrades in the presence of visual occlusions. MACVO is a frame-to-frame stereo odometry. It suffers from sudden viewpoint shifts but still shows exceptional translation accuracy. TartanGround poses a unique challenge for the existing SLAM algorithms, and becomes a good complement to the existing SLAM benchmarks.

### C. Bird’s Eye View Prediction

Bird’s Eye View (BEV) is an efficient way of representing the environments in the top-down view. This representation provides a comprehensive spatial understanding, facilitates the fusion of various sensor modalities, and is easily adaptable for downstream tasks such as object tracking and planning. Networks predicting semantic BEV maps in structured urban environments [38], [39] and predicting elevation and traversability BEV maps in unstructured environments [40]–[42] have gained popularity in recent years. TartanGround, with its diversity and scale, provides an ideal platform to advance these approaches.

### D. Neural Scene Representation

The photorealism of our dataset makes it well-suited for advancing research in neural scene representation techniques, such as Gaussian splatting [43] and NeRFs [44], as well as neural SLAM methods [45]–[48]. Its large-scale scenarios, with dynamic lighting and adverse weather conditions, offer challenging test cases for novel view synthesis and robust scene reconstruction. As shown in Fig. 7, novel view synthesis using Gaussian splatting trained on trajectories from the Rome and CoalMine environments demonstrates the potential of TartanGround for high-fidelity neural rendering.

### E. Navigation

The dataset can be used for various advanced navigation techniques in ground robotics. Recent research has demonstrated the potential of imitation learning and diffusion-based approaches for robust navigation in complex environments. Models such as NoMaD [49], iPlanner [50], and ViPlanner [51] rely on diverse and large-scale datasets for training and evaluation. The TartanGround dataset, with its variety of environments, provides an ideal platform to develop and test these navigation models, enabling the creation of more robust and generalizable navigation systems for ground robots.

## V. CONCLUSION AND FUTURE WORK

In this paper, we introduce TartanGround, a large-scale, multi-modal dataset designed to advance perception and navigation for ground robots in diverse environments. Our evaluations reveal the limitations of existing methods when applied to complex, unstructured environments, emphasizing the need for more robust and generalizable models. By providing comprehensive sensory data including multiple RGB stereo images, depth, semantic labels, LiDAR point clouds, semantic occupancy maps, and ground truth pose, TartanGround provides an ideal platform for training and benchmarking novel methods in occupancy prediction, SLAM, neural scene representation, visual navigation and more. In future, we aim to curate and release task-specific benchmarks utilizing the TartanGround dataset.

### ACKNOWLEDGEMENTS

This work was supported by the Luxembourg National Research Fund (Ref. 18990533) and the Swiss National Science Foundation (Ref. 200021E\_229503). This work used Bridges-2 at PSC through allocation cis220039p from the Advanced Cyberinfrastructure Coordination Ecosystem: Services & Support (ACCESS) program which is supported by NSF grants 2138259, 2138286, 2138307, 2137603, and 2138296. The authors would like to thank Jannick Schröer for generating the Gaussian splatting renderings.

### REFERENCES

- [1] A. Geiger, P. Lenz, C. Stiller, and R. Urtasun, “Vision meets robotics: The kitti dataset,” *The International Journal of Robotics Research*, vol. 32, no. 11, pp. 1231–1237, 2013.
- [2] P. Sun, H. Kretschmar, X. Dotiwalla, A. Chouard, V. Patnaik *et al.*, “Scalability in perception for autonomous driving: Waymo open dataset,” in *IEEE/CVF conference on computer vision and pattern recognition*, 2020, pp. 2446–2454.
- [3] M. Cordts, M. Omran, S. Ramos *et al.*, “The cityscapes dataset for semantic urban scene understanding,” in *IEEE conference on computer vision and pattern recognition*, 2016, pp. 3213–3223.
- [4] H. Caesar, V. Bankiti, A. H. Lang, S. Vora *et al.*, “nuscenes: A multimodal dataset for autonomous driving,” in *Proceedings of the IEEE/CVF conference on computer vision and pattern recognition*, 2020, pp. 11 621–11 631.
- [5] P. Jiang, P. Osteen, M. Wigness, and S. Saripalli, “Rellis-3d dataset: Data, benchmarks and analysis,” in *2021 IEEE international conference on robotics and automation (ICRA)*. IEEE, 2021, pp. 1110–1116.
- [6] M. Wigness, S. Eum, J. G. Rogers, D. Han, and H. Kwon, “A rugd dataset for autonomous navigation and visual perception in unstructured outdoor environments,” in *2019 IEEE/RSJ International Conference on Intelligent Robots and Systems (IROS)*, pp. 5000–5007.

- [7] P. Mortimer, R. Hagmanns, M. Granero, T. Luettel, J. Petereit, and H.-J. Wuensche, "The goose dataset for perception in unstructured environments," in *2024 IEEE International Conference on Robotics and Automation (ICRA)*. IEEE, 2024, pp. 14 838–14 844.
- [8] S. Triest, M. Sivaprakasam, S. J. Wang, W. Wang, A. M. Johnson, and S. Scherer, "Tartandrive: A large-scale dataset for learning off-road dynamics models," in *2022 International Conference on Robotics and Automation (ICRA)*. IEEE, 2022, pp. 2546–2552.
- [9] M. Sivaprakasam, P. Maheshwari, M. G. Castro, S. Triest *et al.*, "Tartandrive 2.0: More modalities and better infrastructure to further self-supervised learning research in off-road driving tasks," *arXiv preprint arXiv:2402.01913*, 2024.
- [10] K. Vidanapathirana, J. Knights, S. Hausler, M. Cox *et al.*, "Wildscenes: A benchmark for 2d and 3d semantic segmentation in large-scale natural environments," *The International Journal of Robotics Research*, p. 02783649241278369, 2024.
- [11] A. Dai, A. X. Chang, M. Savva, M. Halber, T. Funkhouser, and M. Nießner, "ScanNet: Richly-annotated 3d reconstructions of indoor scenes," in *Proceedings of the IEEE conference on computer vision and pattern recognition*, 2017, pp. 5828–5839.
- [12] J. Sturm, N. Engelhard, F. Endres, W. Burgard, and D. Cremers, "A benchmark for the evaluation of rgb-d slam systems," in *International Conference on Intelligent Robot Systems (IROS)*, 2012.
- [13] A. Chang, A. Dai, T. Funkhouser, M. Halber, M. Niessner, M. Savva, S. Song, A. Zeng, and Y. Zhang, "Matterport3d: Learning from rgb-d data in indoor environments," *arXiv preprint arXiv:1709.06158*, 2017.
- [14] W. Wang, D. Zhu, X. Wang, Y. Hu *et al.*, "Tartanair: A dataset to push the limits of visual slam," in *2020 IEEE/RSJ International Conference on Intelligent Robots and Systems (IROS)*.
- [15] Z. Teed and J. Deng, "Droid-slam: Deep visual slam for monocular, stereo, and rgb-d cameras," *Advances in neural information processing systems*, vol. 34, pp. 16 558–16 569, 2021.
- [16] Y. Cabon, N. Murray, and M. Humenberger, "Virtual kitti 2," *arXiv preprint arXiv:2001.10773*, 2020.
- [17] Q. Wang, S. Zheng, Q. Yan, F. Deng, K. Zhao, and X. Chu, "Irs: A large naturalistic indoor robotics stereo dataset to train deep models for disparity and surface normal estimation," in *2021 IEEE International Conference on Multimedia and Expo (ICME)*. IEEE, 2021, pp. 1–6.
- [18] M. Roberts, J. Ramapuram, A. Ranjan, A. Kumar *et al.*, "Hypersim: A photorealistic synthetic dataset for holistic indoor scene understanding," in *Proceedings of the IEEE/CVF international conference on computer vision*, 2021, pp. 10 912–10 922.
- [19] L. Yang, B. Kang, Z. Huang, Z. Zhao, X. Xu, J. Feng, and H. Zhao, "Depth anything v2," *arXiv preprint arXiv:2406.09414*, 2024.
- [20] A. Bochkovskii, A. Delaunoy, H. Germain, M. Santos, Y. Zhou, S. R. Richter, and V. Koltun, "Depth pro: Sharp monocular metric depth in less than a second," *arXiv preprint arXiv:2410.02073*, 2024.
- [21] J. Behley, M. Garbade, A. Milioto, J. Quenzel, S. Behnke, C. Stachniss, and J. Gall, "Semantickitti: A dataset for semantic scene understanding of lidar sequences," in *Proceedings of the IEEE/CVF international conference on computer vision*, 2019, pp. 9297–9307.
- [22] X. Tian, T. Jiang, L. Yun, Y. Mao, H. Yang, Y. Wang, Y. Wang, and H. Zhao, "Occ3d: A large-scale 3d occupancy prediction benchmark for autonomous driving," *Advances in Neural Information Processing Systems*, vol. 36, pp. 64 318–64 330, 2023.
- [23] S. Song, S. P. Lichtenberg, and J. Xiao, "Sun rgb-d: A rgb-d scene understanding benchmark suite," in *Proceedings of the IEEE conference on computer vision and pattern recognition*, 2015, pp. 567–576.
- [24] N. Silberman, D. Hoiem *et al.*, "Indoor segmentation and support inference from rgb-d images," in *Computer Vision—ECCV 2012: 12th European Conference on Computer Vision*. Springer, pp. 746–760.
- [25] H. Zhai, J. Mei, C. Min, L. Chen, F. Zhao, and Y. Hu, "Wildocc: A benchmark for off-road 3d semantic occupancy prediction," *arXiv preprint arXiv:2410.15792*, 2024.
- [26] "Tartanair-v2 dataset," <https://tartanair.org>, accessed: 2025-02-28.
- [27] R. Nunes, J. Ferreira, and P. Peixoto, "Synphorest - synthetic photorealistic forest dataset with depth information for machine learning model training," Mar. 2022. [Online]. Available: <https://doi.org/10.5281/zenodo.6369446>
- [28] R. Hagmanns, P. Mortimer, M. Granero, T. Luettel, and J. Petereit, "Excavating in the wild: The goose-ex dataset for semantic segmentation," *arXiv preprint arXiv:2409.18788*, 2024.
- [29] J. Frey, T. Tuna, L. F. T. Fu *et al.*, "Boxi: Design decisions in the context of algorithmic performance for robotics," *arXiv preprint arXiv:2504.18500*, 2025.
- [30] S. Shah, D. Dey, C. Lovett, and A. Kapoor, "Airsim: High-fidelity visual and physical simulation for autonomous vehicles," in *Field and Service Robotics: Results of the 11th International Conference*. Springer, 2018, pp. 621–635.
- [31] B. Yang, J. Cheng, B. Xue, J. Jiao, and M. Liu, "Efficient global navigational planning in 3-d structures based on point cloud tomography," *IEEE/ASME Transactions on Mechatronics*, 2024.
- [32] P. Fankhauser, M. Bloesch, C. Gehring, M. Hutter, and R. Siegwart, "Robot-centric elevation mapping with uncertainty estimates," in *Mobile Service Robotics*. World Scientific, 2014, pp. 433–440.
- [33] Y. Wei, L. Zhao, W. Zheng, Z. Zhu, J. Zhou, and J. Lu, "Surroundocc: Multi-camera 3d occupancy prediction for autonomous driving," in *Proceedings of the IEEE/CVF International Conference on Computer Vision*, 2023, pp. 21 729–21 740.
- [34] M. Xu, Z. Zhang, F. Wei, H. Hu, and X. Bai, "Side adapter network for open-vocabulary semantic segmentation," in *IEEE/CVF conference on computer vision and pattern recognition*, 2023.
- [35] C. Campos, R. Elvira, J. J. G. Rodríguez, J. M. Montiel, and J. D. Tardós, "Orb-slam3: An accurate open-source library for visual, visual-inertial, and multimap slam," *IEEE transactions on robotics*, vol. 37, no. 6, pp. 1874–1890, 2021.
- [36] L. Lipson, Z. Teed, and J. Deng, "Deep Patch Visual SLAM," in *European Conference on Computer Vision*, 2024.
- [37] Y. Qiu, Y. Chen, Z. Zhang, W. Wang, and S. Scherer, "Mac-vo: Metrics-aware covariance for learning-based stereo visual odometry," *arXiv preprint arXiv:2409.09479*, 2024.
- [38] J. Phillion and S. Fidler, "Lift, splat, shoot: Encoding images from arbitrary camera rigs by implicitly unprojecting to 3d," in *Computer Vision—ECCV 2020: 16th European Conference, Glasgow, UK, August 23–28, 2020, Proceedings, Part XIV 16*. Springer, 2020, pp. 194–210.
- [39] Z. Liu, H. Tang, A. Amini, X. Yang, H. Mao, D. L. Rus, and S. Han, "Befusion: Multi-task multi-sensor fusion with unified bird's-eye view representation," in *2023 IEEE international conference on robotics and automation (ICRA)*. IEEE, 2023, pp. 2774–2781.
- [40] M. Patel, J. Frey, D. Atha, P. Spieler, M. Hutter, and S. Khattak, "Roadrunner m&m - learning multi-range multi-resolution traversability maps for autonomous off-road navigation," *IEEE Robotics and Automation Letters*, vol. 9, no. 12, pp. 11 425–11 432, 2024.
- [41] J. Frey, M. Patel, D. Atha, J. Nubert, D. Fan *et al.*, "Roadrunner-learning traversability estimation for autonomous off-road driving," *IEEE Transactions on Field Robotics*, 2024.
- [42] X. Meng, N. Hatch, A. Lambert, A. Li, N. Wagener, M. Schmittle *et al.*, "Terrainnet: Visual modeling of complex terrain for high-speed, off-road navigation," *arXiv preprint arXiv:2303.15771*, 2023.
- [43] B. Kerbl, G. Kopanas, T. Leimkühler, and G. Drettakis, "3d gaussian splatting for real-time radiance field rendering," *ACM Trans. Graph.*, vol. 42, no. 4, pp. 139–1, 2023.
- [44] B. Mildenhall, P. P. Srinivasan, M. Tancik *et al.*, "Nerf: Representing scenes as neural radiance fields for view synthesis," *Communications of the ACM*, vol. 65, no. 1, pp. 99–106, 2021.
- [45] Z. Zhu, S. Peng, V. Larsson, W. Xu, H. Bao, Z. Cui, M. R. Oswald, and M. Pollefeys, "Nice-slam: Neural implicit scalable encoding for slam," in *Proceedings of the IEEE/CVF conference on computer vision and pattern recognition*, 2022, pp. 12 786–12 796.
- [46] G. Zhang, E. Sandström, Y. Zhang, M. Patel, L. Van Gool, and M. R. Oswald, "Glorie-slam: Globally optimized rgb-only implicit encoding point cloud slam," *arXiv preprint arXiv:2403.19549*, 2024.
- [47] N. Keetha, J. Karhade, K. M. Jatavallabhula, G. Yang, S. Scherer, D. Ramanan, and J. Luiten, "Splatam: Splat track & map 3d gaussians for dense rgb-d slam," in *Proceedings of the IEEE/CVF Conference on Computer Vision and Pattern Recognition*, 2024, pp. 21 357–21 366.
- [48] E. Sandström, G. Zhang, K. Tateno *et al.*, "Splat-slam: Globally optimized rgb-only slam with 3d gaussians," in *Computer Vision and Pattern Recognition Conference*, 2025, pp. 1680–1691.
- [49] A. Sridhar, D. Shah, C. Glossop, and S. Levine, "Nomad: Goal masked diffusion policies for navigation and exploration," in *2024 IEEE International Conference on Robotics and Automation (ICRA)*.
- [50] F. Yang, C. Wang, C. Cadena, and M. Hutter, "iPlanner: Imperative Path Planning," in *Proceedings of Robotics: Science and Systems*, Daegu, Republic of Korea, July 2023.
- [51] P. Roth, J. Nubert, F. Yang, M. Mittal, and M. Hutter, "Viplanner: Visual semantic imperative learning for local navigation," in *2024 IEEE International Conference on Robotics and Automation (ICRA)*. IEEE, 2024, pp. 5243–5249.